Influence of Sodium Oxide on Properties of Fresh and Hardened Paste of Alkali-Activated Blast-Furnace Slag

A. Allahverdi[1], B. Shaverdi[1] and E. Najafi Kani[2]

Received: June 2009, Revised: March 2010 Accepted: September 2010

Abstract: *The aim of this work is to investigate the influence of sodium oxide on properties of fresh and hardened paste of alkali-activated blast furnace slag from Isfahan steel plant. The silica modulus (SiO_2/Na_2O) of activator was adjusted at 0.6 and a number of mixes were designed in such a way to contain different levels of sodium oxide including 1, 2, 3, 4, 5, and 6% by weight of dry slag. The most important physico-mechanical properties of the pastes including workability, initial and final setting times, 28-day compressive strength and efflorescence severity were measured. Suitable mixes were chosen for more studies including compressive strength at different ages, 90-day autogenous and drying shrinkages. According to the results, increasing the sodium oxide content of the mixes results in increased workability, reduced setting times, and higher compressive strength. The results confirm the possibility of achieving 28-day compressive strengths up to 27.5, 50.0 and 70.0 MPa for mixes with sodium oxide content of 1, 2 and 3 wt% respectively. The measured values for autogenous shrinkage were all less than 0.1% and SEM studies showed a significant decrease in pore sizes with increasing sodium oxide concentration from 1 to 2%.*

Keywords: *Blast Furnace Slag, Alkali-Activator, Compressive Strength, Shrinkage.*

1. Introduction

Alkali-activated binders have attracted a huge attention in recent decades, through their potential capability for replacement with Portland cement. Some advantages of these materials are CO_2 emission decreasing, saving energy sources, pollution decreasing and material recovery. One of the most important types of these materials is alkali-activated blast-furnace slag that achieves through activation of ground granulated blast-furnace slag (GGBFS), the waste of the pig iron production process. Utilization of GGBFS is generally in two ways, as a partial replacement for Portland cement and as the basic binder. Since the GGBFS has latent hydraulic properties, in absence of an alkali-activator it shows very weak mechanical behavior for long time periods and there is a need for an activation process in order to gain appropriate mechanical properties in the time durations acceptable for construction industry. Alkali-activator causes accelerated destruction of aluminosilicate bonds of slag and increases the rate of hydration reactions in such a way that desired mechanical strengths are achieved in early times. In two recent investigations, slag was used as an additive for fly ash-based and metakaolin-based geopolymers and it was found that the incorporation of slag could significantly increase the compressive strength of the geopolymer [1, 2]. Different materials such as Portland cement clinker, lime, gypsum and alkali metal hydroxides, carbonates or silicates in either solution or powder form have been used as alkali-activator, so far. However, the most used alkali-activators are sodium hydroxide and sodium silicate (water glass) [3-9]. Several investigations show that increasing the concentration of alkali-activator improves the mechanical strengths [10, 11]. In a research the effect of alkali activator dosage on setting times of sodium silicate-activated slag pastes was investigated. It was concluded that when the alkali activator dosage is higher, both initial and final setting times are shorter [8].

This work is conducted in such a way to explore the suitability of blast furnace slag from Isfahan steel plant for being activated with alkali-

* *Corresponding author. Email: ali.allahverdi@iust.ac.ir*

1 *Cement Research Center, School of Chemical Engineering, Iran University of Science and Technology, Narmak, Tehran, Iran.*

2 *School of Chemical, Petroleum, and Gas Engineering, Semnan University, Semnan, Iran.*

activator and to investigate the influence of sodium oxide on properties of fresh and hardened paste of the binder. Since alkali-activated blast-furnace slag is a highly amorphous material [12-14], X-ray diffractometry is not a suitable technique to study the molecular structure of this material. However, FTIR spectroscopy technique, as remarked by some authors, is accurate to detect small structural changes and hence, is the most appropriate technique to establish structural changes of amorphous aluminosilicate materials [15]. This method is quite cost effective and well sensitive in short-range structural orders [16]. So, FTIR spectroscopy and SEM techniques were used in this investigation to track the molecular and microstructural changes.

2. Experimental Procedure

2.1. Materials

Blast-furnace slag was prepared from Isfahan steel plant and ground in a laboratory ball mill to a Blaine fineness of 320 m^2/kg and a residue of 1.5% by weight on 90 micron sieve. The prepared slag was also characterized for its chemical and mineralogical compositions. The results of chemical composition determined by wet analysis are summarized in table 1.

As seen, this slag is almost neutral with basicity factor $[(CaO + MgO) / (SiO_2 + Al_2O_3)]$ of 1.04. The X-ray diffractometry pattern of the slag sample is shown in figure 1. As expected, the slag sample is mainly amorphous in view of the large widespread diffraction peak centered at $2\theta = 30°$. However, the X-ray pattern also shows a number of sharper reflection peaks corresponding to Calcite ($CaCO_3$), Akermanite (Ca_2MgSiO_7) and Quartz (SiO_2).

Figure 2 shows the FTIR spectrum of the slag. As seen in figure 2, the spectrum shows two strong peaks. One at wave-number about 450 cm^{-1} and the other a very broad peak at wave-numbers centered

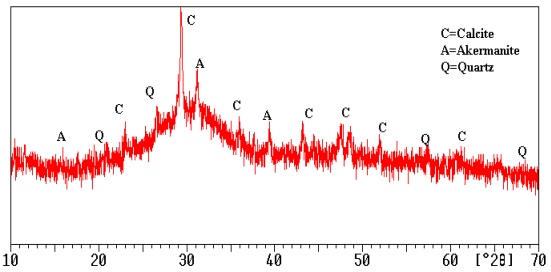

Fig. 1. X-ray diffraction pattern of slag

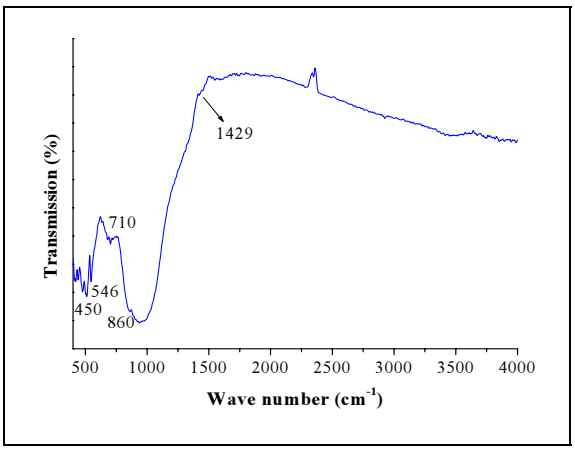

Fig. 2. FTIR spectrum of slag

around 950 cm^{-1} which are attributed to in-plane bending vibrations (ν_2) and asymmetric stretching vibrations (ν_3) of Al-O and Si-O bonds of aluminosilicate structure. Also, weak absorption peaks located at 1429 and 860 cm^{-1} attributed to asymmetric stretching vibrations (ν_3) and out-of-plane bending mode (ν_4) of CO_3^{2-} anions, respectively along with peak at 710 cm^{-1} are characteristics of carbonate compounds (Calcite).

Industrial sodium silicate solution (silica modulus of 0.92 and SiO_2 content of 31.36 wt %) and industrial-grade NaOH (99% purity) were used for preparing activator. Such an activator was also used in previous studies [17,18].

2.2. Synthesis of Alkali-Activated Slag Paste

Enough sodium hydroxide was added to water

Table 1. Chemical composition of Isfahan blast-furnace slag (wt%)

SiO_2	Al_2O_3	Fe_2O_3	CaO	MgO	SO_3	K_2O	Na_2O	TiO_2
36.06	9.16	0.70	36.91	10.21	1.15	0.70	0.48	3.50

Table 2. Chemical composition of mixes

Mix Name	SiO_2/Na_2O ratio (Ms)	Na_2O % (by weight of dry slag)
AS1	0.6	1
AS2	0.6	2
AS3	0.6	3
AS4	0.6	4
AS5	0.6	5
AS6	0.6	6

glass to produce an alkali-activator having a suitable silica modulus (SiO_2/Na_2O), i.e. 0.6, as showing suitable results in previous studies [17]. A number of mixes were designed in such a way to contain different levels of sodium oxide including 1, 2, 3, 4, 5, and 6% by weight of dry slag. The compositions of the mixes are given in table 2. Water-to-dry binder ratio was kept constant at 0.26 for all the mixes.

2.3. Testing Methods

The prepared pastes were firstly characterized for their workability and setting times in accordance with ASTM standards C230 and C191 respectively. To determine the 28-day compressive strength, the prepared pastes were cast into cubic specimens of the size 2×2×2 cm3. The molds were stored at an ambient of more than 95% relative humidity at 25 °C for the first 24 h. After demoulding, specimens were kept in the same ambient up to 28 days. From all the mixes, a 28-day hardened specimen was immersed in 50 ml of distilled water and kept in an open-air atmosphere at ambient temperature of 25 °C until the water was dried completely. The results of efflorescence formation test were obtained qualitatively by just comparing the specimens visually. Mixes showing relatively slight efflorescence formation including those with 1, 2, and 3 wt% sodium oxide were chosen for further measurements including compressive strength at different ages, 90-day autogenous and drying shrinkages, and microstructural and mineralogical studies by means of FTIR spectroscopy and SEM techniques. For measuring the amount of shrinkage, specimens of the size of 2×2×10 cm^3 were prepared and cured in an atmosphere of 95% relative humidity at 25°C for a period of 42 days. During this period, their autogenous shrinkage was measured at the ages of 2, 7, 14, 21, 28, 35, and 42 days. After that, the specimens were taken out of humid atmosphere and held at an open-air atmosphere to measure their drying shrinkage at the ages of 49, 56, 63, 70, 77, 84, and 90 days. The amount of shrinkage was measured using a 0.01 mm accurate caliper. For each measurement of compressive strength and shrinkage, three specimens were used and the average of the three values was reported as the result.

The hardened pastes of the chosen mixes were characterized by the Fourier transform infrared (FTIR) spectroscopy technique. FTIR spectra were collected using an IRsolution 8400S SHIMADZU FTIR spectrometer in transmittance mode from 400 to 4000 cm^{-1} using standard KBr technique. All spectra were obtained with a sensitivity of 2 cm^{-1} and 10 scans per spectrum. Scanning electron microscopy (SEM) was performed using a VEGA II TESCAN (Germany) SEM device with an accelerating voltage of 15 kV.

3. Results and Discussion

3.1. Workability

Figure 3 shows the results obtained for spread diameter as a measure of relative workability. As shown, paste workability increases with sodium oxide concentration so that the paste having 6 wt% of sodium oxide exhibits a considerably higher workability compared to the pastes containing lower concentrations of sodium oxide. This could be attributed mainly to the plasticizing effect of sodium oxide. It could also be claimed that higher sodium oxide concentrations resulting in faster and more dissolution of raw slag phases can probably provide a positive effect on the paste workability. Such a hypothesis, however, needs more detailed investigations to be studied.

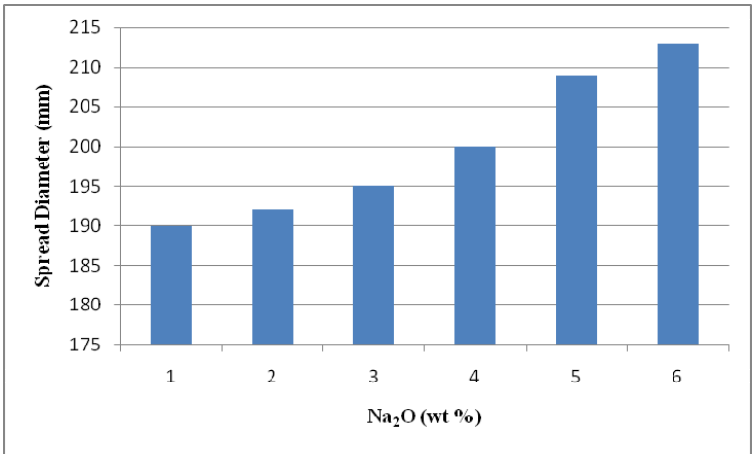

Fig. 3. Spread diameter of pastes versus sodium oxide concentration

3.2. Initial and Final Setting Times

Effect of sodium oxide concentration on initial and final setting times are presented in figures 4 and 5, respectively. As seen, variations of both initial and final setting times with sodium oxide concentration follow very similar patterns. Both setting times decrease with increasing sodium oxide concentration. Initial and final setting times of the pastes, varies in the range between 98 to 320 and 159 to 435 minutes respectively. The minimum and maximum values occur at 6 and 1 wt% Na_2O respectively, showing the governing effect of sodium oxide concentration on the setting times. Since the phenomenon of setting is due to the formation of new compounds exhibiting binding properties, one can conclude that at a constant water-to-dry binder ratio, sodium oxide concentration is the most important factor determining the kinetics of the chemical reactions between alkali-activator and dry binder, i.e. ground slag.

The minimum initial and maximum final acceptable setting times given in ASTM C191 for Portland cement paste prepared with an amount of water content producing standard consistency are 45 and 375 minutes. Now as seen, most of the results obtained for alkali-activated slag pastes are acceptable compared to the given limits. A number of pastes with activators having a sodium oxide content less than 3 wt% exhibit slow setting behavior.

3.3. 28-Day Compressive Strength

Results of 28-day compressive strength test are shown in figure 6. As seen, compressive strength

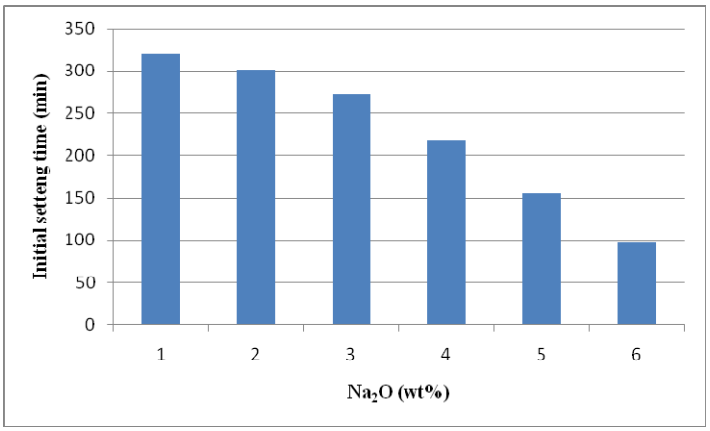

Fig. 4. Initial setting times versus sodium oxide concentration

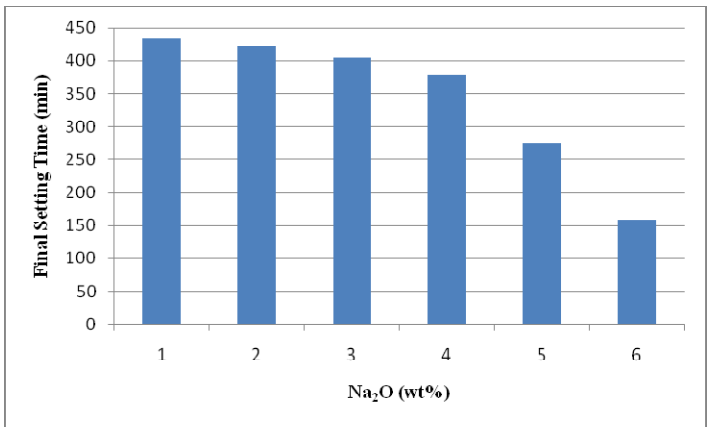

Fig. 5. Final setting times versus sodium oxide concentration

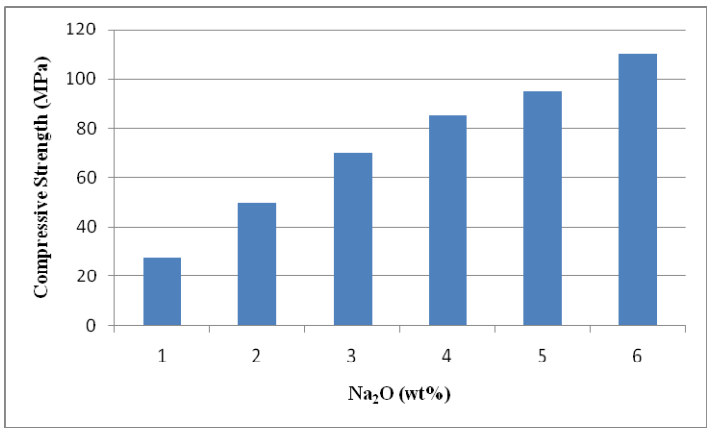

Fig. 6. 28-day compressive strength versus sodium oxide concentration

significantly increases with increasing sodium oxide concentration. The minimum and maximum values of 28-day compressive strengths are 28.0 and 110.0 MPa obtained at sodium oxide concentrations of 1 and 6 wt% respectively. Such compressive strengths are high enough to be comparable to that of Portland cement paste. These results are in agreement with those published previously [10, 11]. Again, the reason can be attributed to the effective and significant role of sodium oxide concentration in cementing reactions progressing in the slag media during the course of activation. In other word, a higher concentration of sodium oxide produces a stronger alkaline media and causes a higher amount of slag to be involved in the cementing reactions at a given time. As a result, higher proportions of slag are dissolved which in turn result in the formation of higher amounts of binding compounds and hence exhibiting a stronger compressive strength behavior.

3.4. Efflorescence

Figure 7 shows the severity of the efflorescence formation in all the six mixes qualitatively. Specimens of mixes containing 1, 2 ..., 6 wt% sodium oxide are represented by labels A, B ..., D respectively. As seen, efflorescence severity is intensifying with increasing sodium oxide concentration. Three different grades of relative efflorescence severity were defined based on the test results. The severity of the efflorescence has been classified in three different relative grades of slight, moderate, and severe. According to visual observations, mixes with 1 and 2 wt% sodium oxide concentration lie in the grade of slight efflorescence formation, whereas mix containing 3

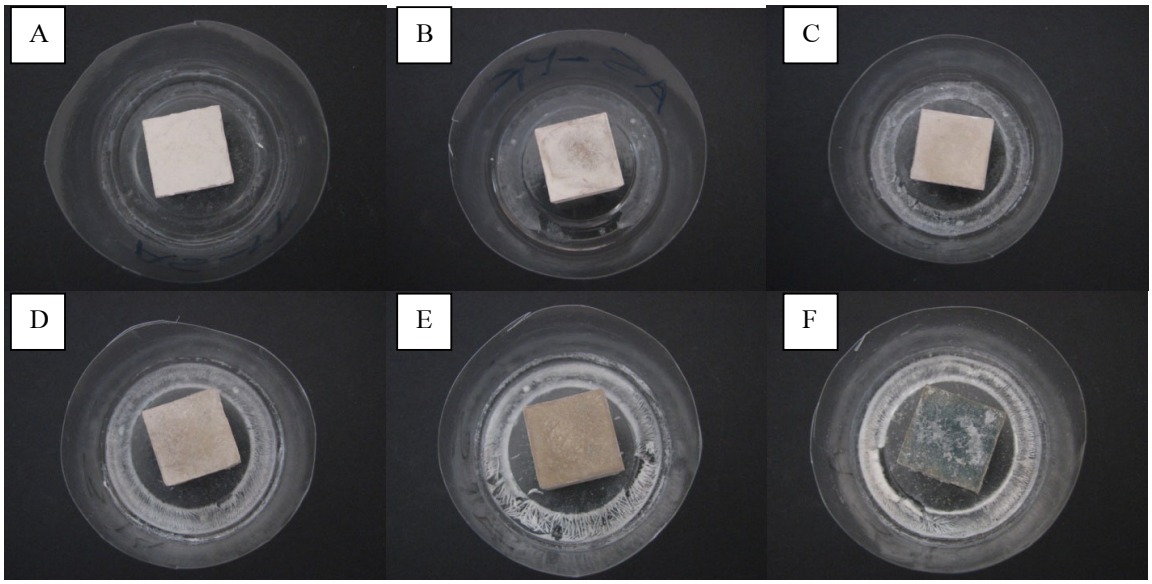

Fig. 7. Specimens subjected to efflorescence test with sodium oxide concentration of 1 wt% (A), 2 wt% (B), 3 wt% (C), 4 wt% (D), 5 wt% (E), and 6 wt% (F)

wt% sodium oxide is categorized in grade moderate. Mixes containing higher concentrations of sodium oxide, i.e. 4, 5, and 6 wt%, are those exhibiting severe efflorescence and therefore considered in grade sever.

These observations clearly confirm the relation between the severity of the efflorescence and the concentration of sodium oxide. A relatively high concentration of sodium oxide could be partially in excess and results in some non-reacted sodium hydroxide in the material which can be easily leached out. The leached sodium hydroxide reacts with atmospheric carbon dioxide to produce sodium carbonate and to result in efflorescence formation.

Based on the above results, mixes with slight and moderate efflorescence, i.e. those with 1, 2, and 3 wt% sodium oxide concentration, were chosen for further investigations.

3.5. Different Age Compressive Strengths

Compressive strength of selected mixes was measured at different ages of 2, 7, 14, 21, 28, 50, 90, 120, 150 and 180 days after molding. Storage condition was quite similar to what applied for 28-day compressive strength test. Figure 8 shows the results obtained representing the rate of

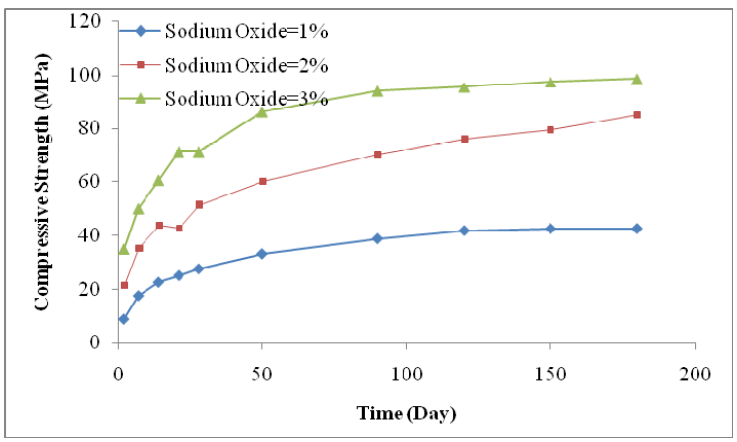

Fig. 8. Compressive strength versus curing time

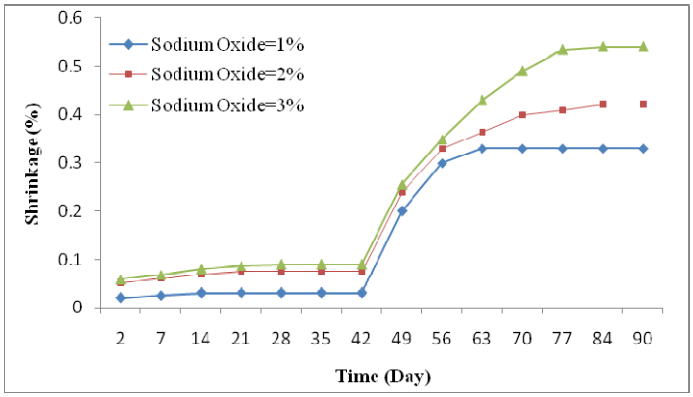

Fig. 9. Shrinkage development versus sodium oxide concentrations

strength gain versus curing time. As seen, at a constant sodium oxide concentration, compressive strength increases with curing time. The increment is more significant in earlier times and from 28th day forward the rate of compressive strength development slowdowns. The effect of sodium oxide concentration on increase of compressive strength is well evident in figure 8. Such a result was also reported previously [19]. The 180-day compressive strengths are 42.0, 85.0 and 99.0 MPa for sodium oxide concentrations of 1, 2 and 3 wt% respectively.

3.6. Shrinkage

Mixes with slight and moderate efflorescence, i.e. those with 1, 2, and 3 wt% sodium oxide, were also submitted to shrinkage test. The amount of shrinkage was measured at certain ages as a percentage of the initial length. The results obtained are presented graphically in figure 9. As seen in figure 9, increasing sodium oxide concentration results in increasing both autogenous and drying shrinkages. The general trends of current results are in good agreement with those reported by Melo Neto et al. [20]. Both autogenous and drying shrinkage amounts approach their final values during the early ages. As seen, for all mixes total autogenous shrinkage is quite less and below 0.1%. Moreover, for specimens including 2 and 3 wt% sodium oxide, autogenous shrinkage reaches its final value after almost three weeks. However, for specimens containing 1 wt% sodium oxide this stage lasts around only one week. This dissimilarity demonstrates that in specimens with 1 wt% sodium oxide the hydration reactions take place to a lower extent and as a result, fewer amounts of hydration products are produced. According to some recent research results [11, 20, 21], mechanical properties, porosity and degree of hydration, which are determining factors for the evolution of autogenous shrinkage are greatly influenced by the amount of activator.

After 42 days, the specimens were taken to an open-air atmosphere for being dried. A sharp slope increase was observed during the first two weeks of drying period for specimens with 1 wt% sodium oxide. At the age of 56 days, these specimens show a shrinkage amount of 0.3%. Afterwards, shrinkage growth becomes very slow up to the age of 90 days. For specimens with 2 and 3 wt% sodium oxide, drying shrinkage grows fast up to 4 weeks of exposure and then, the rate diminishes. For mix with 2 wt% sodium oxide, shrinkage reaches to maximum amount of almost 0.42%. Mix with 3 wt% sodium oxide exhibits the highest growth in shrinkage reaching values up to 0.54% during the same time.

An important point to mention is the relative share of autogenous volume changes in the total 90-day shrinkage. As seen in figure 9, in all mixes the contribution of total autogenous shrinkage occurring up to 42 days, at the highest value is even less than 17% of total shrinkage. This confirms that the volume changes brought about by the effect of cementing reactions are not very appreciable in comparison with volume changes brought about by evaporation of free

water. The amounts of total 90-day shrinkages are all practically acceptable compared to those usually reported for Portland cement pastes.

3.7. FTIR Spectroscopy

FTIR spectra of 40-day hardened pastes containing 1, 2, 3 and 6 wt% sodium oxide are shown in figure 10. As seen, all the spectra are very similar, having analogous absorption bands. All of them have bands around 3440 and 1650 cm^{-1} attributed to O-H stretching and bending modes of molecular water, respectively. Also, the bands around 960 and 450 cm^{-1} are due to asymmetric stretching vibrations (v_3) of Si—O(Al) and in-plane bending vibrations (v_2) of Si—O in SiO_4 tetrahedral, respectively. All samples have carbonate compounds, presenting a strong absorption band around 1450 cm^{-1} and a small one at 870 cm^{-1} due to asymmetric stretching vibrations (v_3) and out-of-plane bending vibrations (v_4) of CO_3^{2-} anions [12]. The broad band around 1450 cm^{-1}, due to anti-symmetric stretching vibrations of CO_3^{2-} ions, is a result of the presence of sodium carbonate (Na_2CO_3) [22-25] generated from carbonation of excess sodium oxide, arisen from alkali-activator, at the external layers of specimen, known as efflorescence. Observation of the efflorescence on the surfaces of specimens is evidence of this claim. Broadness of the main absorption band around 960 cm^{-1} is indicative of disordered structure of these materials. The Si-O stretching vibrations for the SiQ^n units show IR absorption bands located around 1100, 1000, 950, 900, and 850 cm^{-1} for n = 4, 3, 2, 1, and 0, respectively [22]. According to this, broadness of the main band is resulted from coexistence of various SiQ^n units in the structure of 40-day hardened paste. These values shift to lower wave-numbers when the degree of silicon substitution by aluminum in the second coordination sphere increases, as a consequence of the weaker Al-O bonds [23].

It can be seen from Figure 10 that increasing sodium oxide concentration from 2 to 6 wt%, results in shifting the main band from 960 to 966 cm^{-1}. This could be as a result of increasing Q^3 units. However, 1 wt% sodium oxide is exclusion and the main band shifts to higher wave-numbers

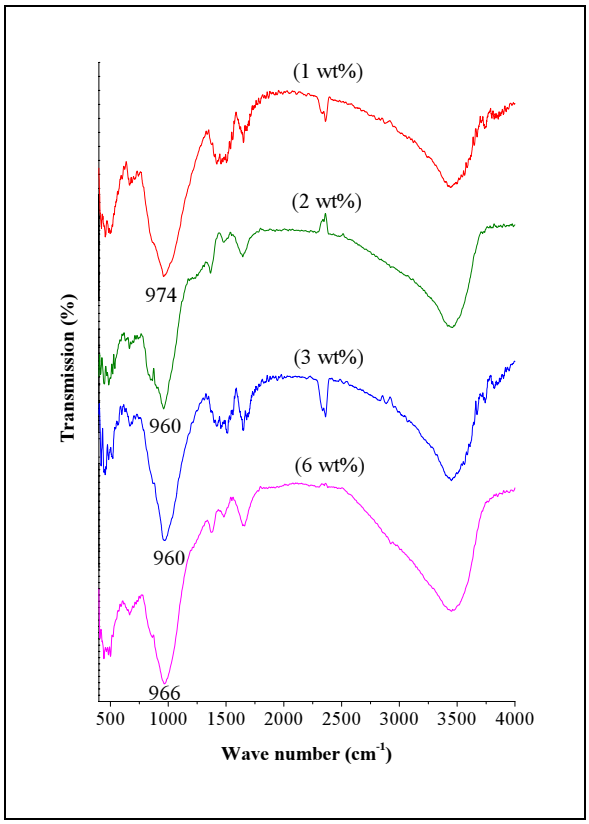

Fig. 10. FTIR spectra of 40-day hardened pastes of mixes with 1, 2, 3 and 6 wt% sodium oxide

in spite of decreasing sodium oxide concentration. This could be resulted from decreasing the degree of silicon substitution by aluminum as well as decreasing the amount of sodium ions in the structure of hydration products, as a result of less extension of hydration reactions and of decreasing amount of sodium ions in the primary activated slag paste, respectively. Consequently, silicon amount relatively increases in the structure of hydration products, resulting in shifting the main band to higher wave-numbers. The infrared spectra presented in figure 10 shows some differences in comparison with the spectrum of the initial slag sample (figure 2). The main absorption band has been much more concentrated in 40-day hardened pastes, showing that the hydration reactions have resulted in a more oriented molecular structure. In addition, this main peak has shifted to higher wave-numbers in 40-day hardened confirming that the hydration reactions have resulted in a higher degree of polymerization and hence, in a stronger structure.

Moreover, the strong absorption band around 1450 cm^{-1}, attributed to formation of sodium carbonate salt (efflorescence phenomenon) is appeared in the spectrum of alkali-activated slag. No footprint from characteristic bands of molecular water bonds can be seen in the spectrum of slag sample.

3.8. SEM Analysis

In order to investigate the effect of sodium oxide concentration on the microstructure of the 40-day hardened slag pastes, SEM microscopy was performed on samples containing 1 and 2 wt% sodium oxide. Micrographs of these samples are shown in figures 11(A) and 11(B), respectively. As seen, slag particles have different shapes and sizes including coarse particles with sharp corners, well apparent in figure 11(A). Since these particles maintain their shapes in a wide range, it could be concluded that they have not been involved in cementing reactions very well. Slag particles are surrounded by a cementing matrix of reaction products in figure 11(B); however, figure 11(A) shows only a rather narrow layer of reaction products on the surface of slag particles and among them, which adheres slag particles together. A high content of pore volumes of large size in the microstructure of hardened slag paste is well understood from figure 11(A). This could be resulted through the unsuitable involvement of slag grains in cementing reactions, which causes the voids among the slag particles to be not filled. As seen in figure 11 (B), fine slag particles are disappeared or deformed to a great extent and cementing products have formed a relatively homogeneous matrix. However, coarse slag particles have not involved in cementing reactions to a great extent and have maintained their shape, yet. It could be seen that increasing sodium oxide concentration from 1 to 2 wt% have refined the microstructure of the hardened paste and considerably decreased the pore volume and size, as a result of significant increase of slag reactivity and hence, formation of higher amounts of reaction products. This matter could explain compressive strength increase due to increasing sodium oxide concentration. A number of heterogeneous micro-cracks, which could not be due to specimen preparation for SEM studies, are shown in figure 11(B). Clearly, presence of these micro-cracks could itself diminish the compressive strength. Therefore, any factor preventing formation of these micro-cracks, or eliminating them, could

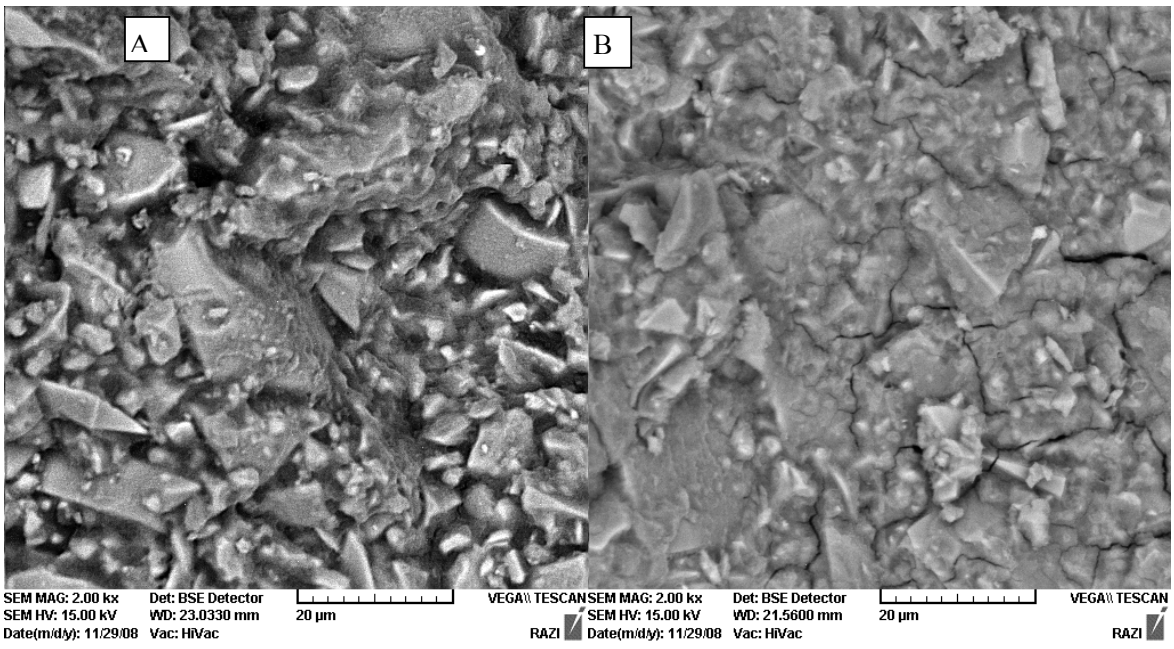

Fig. 11. SEM micrographs of 40-day hardened pastes of mixes containing 1 (A) and 2 (B) wt% sodium oxide

improve the mechanical behavior. These observations show that 40-day hardened paste containing 1 wt% sodium oxide has a weak and unsuitable microstructure containing a high content of pore volume of relatively large sizes, susceptible to external attacks. The other specimen with a rather homogeneous matrix, however, has a much lower pore volume with very smaller size range, which is not observable at the scale of the image.

4. Conclusions

1. Alkali-activation of the blast-furnace slag from Isfahan steel plant resulted in a number of workable pastes with Initial and final setting times generally acceptable comparing with those attributed to Portland cement. Increase of the sodium oxide concentration increases workability and decreases both initial and final setting times of the pastes.
2. Mixes with 1 and 2 wt% sodium oxide show a relatively slight efflorescence formation.
3. Compressive strength increases significantly with increasing sodium oxide concentration and 180-day compressive strengths up to 42.0, 85.0 and 99.0 MPa are achievable for mixes containing 1, 2 and 3 wt% sodium oxide, respectively.
4. Both autogenous and drying shrinkages increase with increasing sodium oxide concentration. For all mixes total autogenous shrinkage is quite less and below 0.1%. Total 90-day shrinkages are all practically acceptable compared to those usually reported for Portland cement pastes.
5. According to microanalysis studies, hydration reactions have resulted in a more oriented molecular structure with a higher degree of polymerization. Increasing sodium oxide concentration from 1 to 2 wt% has a considerable refinement effect on micro-structure of 40-day hardened slag paste.
6. The mix composed of 2 wt% sodium oxide is the most favorable one with the best total properties, such as good mechanical behavior, slight efflorescence and suitable microstructure.

References

[1] Li Z. and Liu S.: 2007, Influence of slag as additive on compressive strength of fly ash-based geopolymer, J. Mat. Civ. Eng. 19(6), 470-474.

[2] Soare, L.C. and Garcia-Luna, A.: 2008, Synthesis and characterization of inorganic polymer cement from metakaolin and slag, Ceram. Eng. Sci. Proc. 28(9), 283-292.

[3] Palacios, M. and Puertas, F.: 2007, Effect of shrinkage-reducing admixtures on the properties of alkali-activated slag mortars and pastes, Cem. Conc. Res. 37, 691–702.

[4] Palacios, M. and Puertas, F.: 2005, Effect of superplasticizer and shrinkage-reducing admixtures on alkali-activated slag pastes and mortars, Cem. Conc. Res. 35, 1358–1367.

[5] Puertas, F., Fernandez-Jimenez, A. and Blanco-Varela, M.T.: 2007, Pore solution in alkali-activated slag cement pastes. Relation to the composition and structure of calcium silicate hydrate, Cem. Conc. Res. 37, 691–702.

[6] Pan, Z., Li, D., Yu, J. and Yang, N.: 2003, Properties and microstructure of the hardened alkali-activated red mud–slag cementitious material, Cem. Conc. Res. 33, 1437–1441.

[7] Qian, G., Sun, D.D. and Tay, J.H.: 2003, Characterization of mercury- and zinc-doped alkali-activated slag matrix Part I. Mercury, Cem. Conc. Res. 33, 1251–1256.

[8] Chang, J.J.: 2003, A study on the setting characteristics of sodium silicate-activated slag pastes, Cem. Conc. Res. 33, 1005–1011.

[9] Holloway, M. and Sykes, J.M.: 2005, Studies of the corrosion of mild steel in alkali-activated slag cement mortars with sodium chloride

admixtures by a galvanostatic pulse method, Corr. Sci. 47, 3097–3110.

[10] Allahverdi, A., Mehrpor, K., and Najafi Kani, E.: 2008, Investigating the Possibility of Utilizing Pumice-Type Natural Pozzolan in Production of Geopolymer Cement, Ceramics-Silikaty 52(1), 16-23.

[11] Atis, C.D., Bilim, C., Çelik, Ö. and Karahan, O.,: 2009, Influence of activator on the strength and drying shrinkage of alkali-activated slag mortar, Cons. Build. Mat. 23, 548–555.

[12] Lecomte, I., Henrist, C., Liegeois, M., Maseri, F., Rulmont, A. and Cloots, R.: 2006, (Micro)-structural comparison between geopolymers, alkali-activated slag cement and Portland cement, J. Euro. Ceram. Soc. 26, 3789–3797.

[13] Zhang, Y.J., Zhao, Y.L., Li, H.H. and Xu, D.L.: 2008, Structure characterization of hydration products generated by alkaline activation of granulated blast furnace slag, J. Mater. Sci. 43, 7141–7147.

[14] Khale, D. and Chaudhary, R.: 2007, Mechanism of geopolymerization and factors influencing its development: a review, J. Mater. Sci. 42, 729–746.

[15] Lee, W.K.W. and Van Deventer, J.S.J.: 2002, The effects of inorganic salt contamination on the strength and durability of geopolymers, Colloids and surfaces 211, 115–126.

[16] Farmer, V.C.: 1974, The Infrared Spectra of Minerals, Mineralogical Society, London.

[17] Allahverdi, A., Najafi Kani, E. and Esmaeilpoor, S.: 2008, Effects of Silica Modulus and Alkali Concentration on Activation of Blast-Furnace Slag, Iranian J. Mater. Sci. Eng. 5(2), 32-35.

[18] Allahverdi, A., Najafi Kani, E.: 2009, Construction Wastes as Raw Materials for Geopolymer Binders, International Journal of Civil Engineerng. 7(3), 154-160.

[19] Krizan, D. and Zivanovic, B.: 2002, Effects of dosage and modulus of water glass on early hydration of alkali-slag cements, Cem. Conc. Res. 32, 1181–1188.

[20] Melo Neto, A.A., Cincotto, M.A. and Repette, W.: 2008, Drying and autogenous shrinkage of pastes and mortars with activated slag cement, Cem. Conc. Res. 38, 565-574.

[21] Cincotto, M.A., Melo Neto, A.A. and Repette, W.L.: 2003, Effect of different activators type and dosages and relation with autogenous shrinkage of activated blast furnace slag cement, proceedings of International Congress on the Chemistry of Cement, 1878–1888.

[22] Clayden, N.J., Esposito, S., Aronne, A., and Pernice, P.: 1991, Solid state 27Al NMR and FTIR study of lanthanum aluminosilicate glasses, J. Non-Cryst. Solids 11, 258-268.

[23] Ortego, J.D., and Barroeta, Y.: 1991, Leaching effects on silicate polymerization, A FTIR and 29Si NMR study of lead and zinc in Portland cement, Environ. Sci. Technol. 25, 1171– 1174.

[24] Phair, J.W. and Van Deventer, J.S.J.: 2002, Effect of the silicate activator pH on the microstructural characteristics of waste-based geopolymers, Int. J. Miner. Process. 66, 121–143.

[25] Swanepoel, J.C. and Strydom, C.A.: 2002, Utilisation of fly ash in a geopolymeric material, Applied Geochemistry 17, 1143–1148.